Jestr

Journal of Engineering Science and Technology Review 16 (4) (2023) 127 - 132

Research Article

JOURNAL OF
Engineering Science and Technology Review

www.jestr.org

A Compact Four-Port MIMO Antenna Using Cylindrical Dielectric Resonators for Millimetre Wave Applications

Upali Aparajita Dash[1,*], Sasmita Pahadsingh[2], Bhargav Appasani[2] and Gangadhar Mishra[1]

[1]*KIIT Polytechnic, Bhubaneswar, Odisha*
[2]*KIIT Deemed to be University Bhubaneswar, Odisha*

Received 15 April 2023; Accepted 5 September 2023

Abstract

A four-port Multiple Input Multiple Output (MIMO) system consisting of Cylindrical Dielectric Resonator Antennas (CDRA) is investigated for millimetre wave applications. The proposed design comprises four CDRAs on a single compact substrate and is excited by aperture coupling with orthogonal feeding arrangement and ground plane modification. The combined effect of both the arrangements offers the desired inter port isolation and gain improvement. The MIMO CDRA prototype is fabricated having a compact volume of $8\times 8\times 6$ mm^3, resonating at 40 and 45 GHz. The peak gain of the antenna is 7.9 dBi at 40 GHz. The measurement results are in good agreement with the simulation results. Additionally, the MIMO system is analyzed for its Isolation, Envelope correlation coefficient (ECC), mean effective gain (MEG) and diversity gain (DG). The inter port isolation is -30 dB supported with permissible limit of .05 and 10 dB of ECC and DG respectively. The designed compact structure can find potential practical applications in high frequency MIMO communication.

Keywords: MIMO, Millimetre wave, Cylindrical DRA.

1. Introduction

The unlicensed band of 40 GHz has received significant attention from the research fraternity. However, this band's signal loss is significant due to atmospheric absorption. The lower interference and greater frequency reuse can overcome this drawback of atmospheric absorption. The concept of frequency reuse leads to the advancement of wireless technology, which has increased the extent and fidelity requirement for the millimetre wave application these days. With one input and one output arrangement, it is impossible to meet the advanced communication requirements because of limited channel capacity and data rate [1]. Multiple-input-multiple-output (MIMO) technology attracted many researchers to meet these advanced demands. This multiple port technique helps to deliver several samples of the uncorrelated wave with equal power amplitude by using numerous elements on the transmission and reception sides [2-4]. The compact MIMO antenna operates at higher frequency providing high transmission rate with greater immunity to interference. In this regard, many planar antennas are effectively used for MIMO systems because of their easy integration into portable devices. However, at high frequencies, the metallic losses in the planar antenna microstrip patch become acute. At the same time, DRAs proved to be a good replacement for patches for decades due to their attractive features like high impedance bandwidth, high radiation efficiency and high gain [7][8].

Many earlier investigated works on MIMO using DRA for millimetre wave applications have been implemented in the literature. A MIMO antenna using cylindrical DRAs is reported to operate at 30 GHz. Beam tilting is used for desired phase excitation and reduction of mutual coupling. The antenna exhibits good MIMO performance parameters in millimetre-wave applications [9]. Another work suggests that a two port MIMO antenna using rectangular DRA can be a good candidate for millimeter wave application at 26 GHz by adding metal vias [10]. The metal vias help to vary the field distribution and reduce the coupled fields. A well-designed planar array using cylindrical DRA can resonate 69.5 to 90.97 GHz with multi-feeding inputs [11]. A four-port millimetre wave MIMO antenna excited with individual microstrip feed line resonates at 28 GHz band with defected ground structure is etched on the substrate to enhance the inter port isolation and makes it suitable for 5G application [12]. Another work depicts that two four-element DRA array antennas can serve two port MIMO configurations by steering the beam electronically. The array elements are fed by massive microstrip feed lines to resonate in the 30 GHz band [13]. A novel work suggesting four port MIMO consisting of rectangular DRA on the surface Integrated Surface (SIW) can resonate at 28 GHz.

The mode excitation in the rectangular DRA due to slotted feed helps efficient broadside radiation with improved isolation [14]. Each DR element is coated with a metal strip to cover a band of 27.5-28.35 and efficiently create isolation [15]. Also, printing metamaterial on the DRA body helps to interact with electromagnetic fields and create isolation in the band 26.71-28.9[16]. The metasurface comprising of SRR helps to get band stop functionality. Reduced coupling level is achieved significantly by not compromising the antenna performance [17]. Another work suggests two linear arrays comprising four DRAs for each MIMO configuration. The array configuration having a fixed direction of the beam is tilted to reduce mutual coupling in 29.6-31.5 GHz [18]. A couple of rectangular DRAs are fed with a coplanar

*E-mail address: udashfet@kp.kiit.ac.in
ISSN: 1791-2377
doi:10.25103/jestr.164.16

waveguide to resonate at 28 GHz and 38 GHz. The etching of the slot helps improve the isolation to a greater level [19].

The approaches suggested in the above section have higher electrical dimension as per the resonance frequency. Also, the inter port isolation is good with greater sized substrate, but with decrease of dimension the mutual coupling among the antenna elements is elevated. With higher dimension and less inter-port isolation in the MIMO antennas, the capacity of terrestrial wave communication in millimeter wave band is disturbed.

Motivated by these limitations, the current work aims to develop a unique compact four-port merged cylindrical DRAs with a technically modified exciting mechanism. Simultaneously the gain and reasonable inter port isolation also need to be improved with the help of DRAs as an integrated antenna. The feeding mechanism with DRA loading is most effectively realized on a modified ground structure. The prime objective of this research work is to get in high touch with a millimetre wave application antenna on a closed pack volume with superior inter port isolation, improved gain and capacity enhancement. The altered feeding technique using slots helps to achieve hybrid fundamental mode excitation of cylindrical DRA with modified ground structure and minimizes the cross-polarisation and mutual coupling simultaneously. Further, the MIMO behaviour grades are investigated to authenticate the MIMO execution in huge multipath fading surroundings. With this novel design step, the author emphasizes offering some new suggestions for sustaining millimetre wave applications in a wireless environment.

2. Antenna Design

The proposed antenna is depicted in Figure 1 with a dimension of 8 x 8 mm^2. The complete design is fabricated on a Roger substrate with a dielectric constant 2.5, thickness 0.381 mm and loss tangent 0.0015. The Roger substrate helps with low electrical loss and better handling of impedance with the feeding mechanism. The antenna design is initiated with an efficient feeding mechanism of slotted microstrip line loaded with cylindrical Dielectric Resonators. A cylindrical DRA of Eccostock dielectric material (HIK) with dielectric constant 10, loss tangent 0.003, radius 1.5 mm, height 6 mm is integrated on the slotted feed. The Eccostock dielectric has properties of high thermal insulation and low water absorption. Initially, the performance was observed with two ports; then, four ports were developed with individual orthogonally loaded DRAs, as shown in Figure 1. The ground plane is modified orthogonally to accommodate the four cylindrical DRAs. The orthogonal positioning of DRAs on slotted microstrip feed lines with a combination of modified ground plane help to reduce mutual coupling between the elements of the MIMO antenna and provide good isolation. Figure 1 a & b shows the loading of cylindrical DRAs from the top and side view. Figure 1 c & d depicts orthogonally placed slotted feed lines and the 3D view of dielectric loadings on the slotted feed.

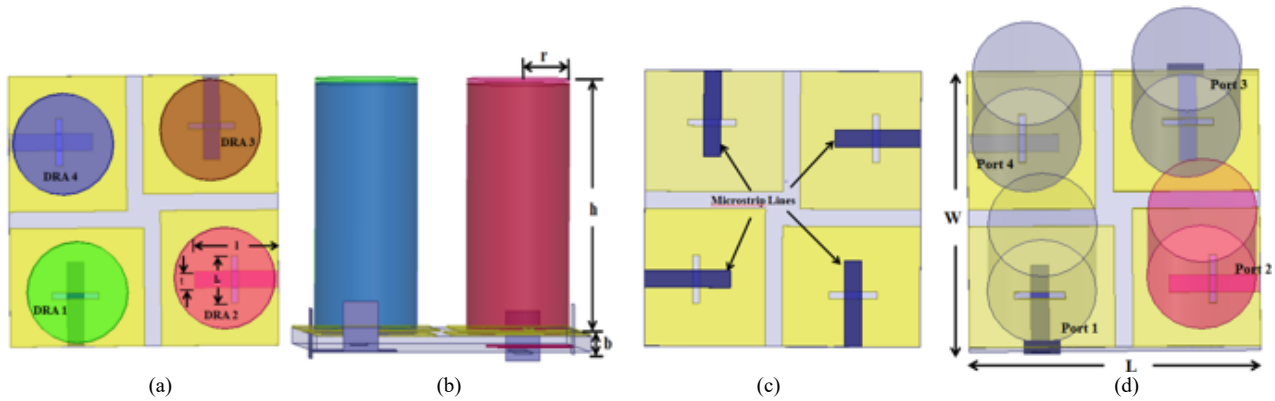

Fig. 1. Design of proposed model (a) Top view (b) Side view (c) Bottom view (d) 3D view.

3. Simulated and Measured Result Analysis and Discussion

3.1. Simulated S - Parameter

The modelling and simulation of the proposed design is carried out using the commercially available simulation software HFSS 14.0. For a better understanding of the modelling technique, three dissimilar layouts of the element design are simulated and analyzed. The first one is with a single port and single DRA of the optimized dimension. The single DRA resonates at 40 GHz with a low coupling of -18 dB. The second approach was to simulate two port DRA with orthogonal microstrip aperture feed. The dual DRA two-port MIMO antenna operates in the 35 GHz - 42 GHz band, resonating at 40 GHz. The MIMO characteristics and gain were reasonably good, as depicted in Figure 2(a & b). However, for better performance, the ultimate aim of the proposed design is to improve the isolation between three ports having less envelope correlation coefficient (ECC) and enhancement in strength. So, the transmission and reflection parameters of the proposed four-port integrated antenna are shown in Figure 2(c).

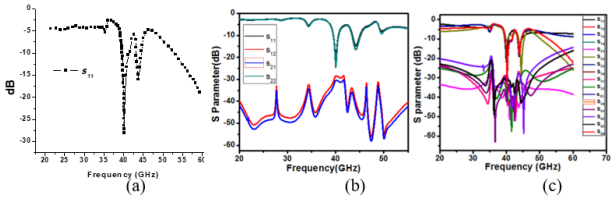

Fig. 2. Simulated S parameter of proposed MIMO model (a) Single port (b) Dual Port (c) Four Port.

3.2. Simulated Radiation Pattern Analysis

An observation from Figure 3 shows that the four-port MIMO depicts a good separation between co-polarisation and cross-polarization radiation characteristics. For 40 GHz, the cross-polarisation separation in 4 port MIMO, it is -30 dB and the co-polarisation gain is around 8 dBi. However, at 45 GHz the pattern leads to distortion which is the result of phase difference due to different paths of reduced wavelength. The simulation fact on co-polarisation can be validated with the simulated gain plots.

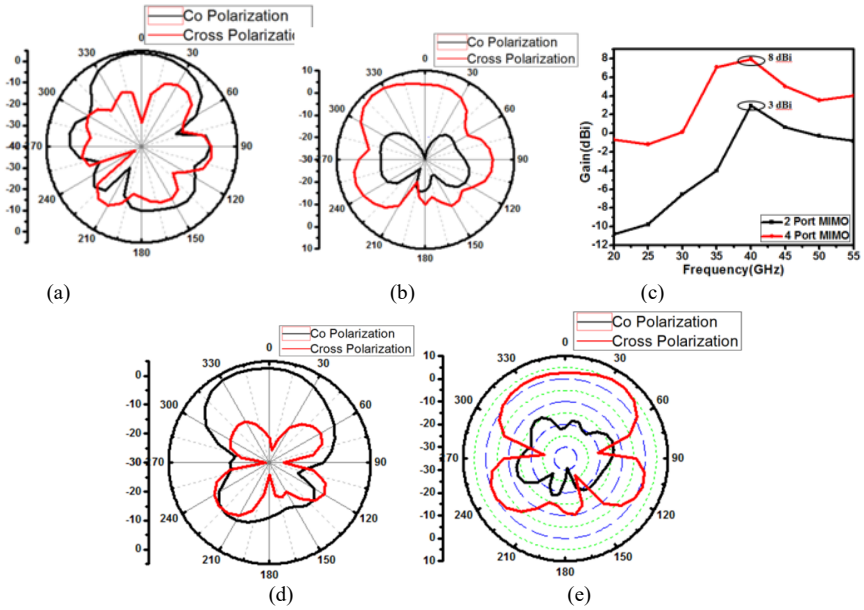

Fig. 3. Simulated Results (a) & (b) Radiation pattern at 40 GHz (c) Gain at 40 GHz (d) & (e) Radiation pattern at 45GHz

4. Fabrication and Measurement Result Analysis

The fabrication and measured results validate the optimized 4 port MIMO antenna. The model is fabricated, and Agilent's E8363B Network Analyzer is used to measure radiation pattern at 40 GHz. Figure 4(a-d) shows the fabrication model prototype and setup for measurement of reflection coefficient (S_{11}) and radiation pattern.

Fig 4. Fabrication of prototype model (a)Top view of a substrate showing slot (b) DRA loaded on slotted patch(c)Model with connectors of VNA (d) R adiation pattern measurement.

4.1. Measured S Parameter Analysis

The s_{11}, s_{22}, $s_{33}$and s_{44} are measured and depicted in Figure 5(a). It is seen that port 3 is homogeneous with port 1and port 4 is similar to port 2. So, s_{11} achieves almost similar behaviour to $s_{33,}$ and s_{22} performs equally to the maximum extent of s_{44}. The isolation in the case of the MIMO diversity radiator amidst all antennas has a vital role. So, separation upliftment with numerous methods in a compact area is a stimulating reality for more than one port modelling. Here, the inter port separation is effectively enhanced using orthogonality in feeding Cylindrical DRA. The coefficient of transmission among different antenna elements after the measurement is shown in Figure 5 (b). The isolation between port1 and port4 is as high as -65 dB, which is significant.

The measurement of the radiation pattern by terminating other ports was not simple due to the chances of breaking the prototype model. It is very small in size and connectors are connected from four sides. However, the measurement of co-polarisation and cross-polarisation in E-plane and H-plane is in good agreement with the simulation result. The broadside radiation in H-plane shows a peak gain of 7dBi and there is visible isolation between co-polarisation and cross-polarisation magnitude with a null visible at $\theta=180^0$. The radiation pattern at 45 GHz was not measured as it requires the same bench setup and reveals an approximately same pattern in the pair of E plane and H plane as depicted in Figure 6(a). The gain after measurement in the resonating span of the band is depicted in Figure 6(b). The measured gain at 40 GHz is 7.19 dBi, closer to the simulated 7.9 dBi. However, the gain after the measurement is 4.8 dBi at 45 GHz, compared to 5.2 dBi of the simulated result. The measurement result differs slightly with the simulation result due to the adhesive used to fix the DRAs on the ground plane. There is a measurement uncertainyty of $\pm$ 0,2 dB at 95 % confidence level. The stated uncertainty is rated at 32 dB. At the measured gain range less than 9dB the error is quite small to have a potential impact.

4.2 Measured Radiation Pattern and mode diagrams

As shown in Figure 7, the mode excitation is $HEM_{11\delta}$ in the CDRA body at 40 GHz. At 45 GHz, the mode is similar to $HEM_{11\delta,}$ with better current concentration to witness the fundamental mode. The proposed work is compared with those in the literature, as shown in Table 2. The proposed MIMO antenna system is compact and yields better inter port isolation with improved gain.

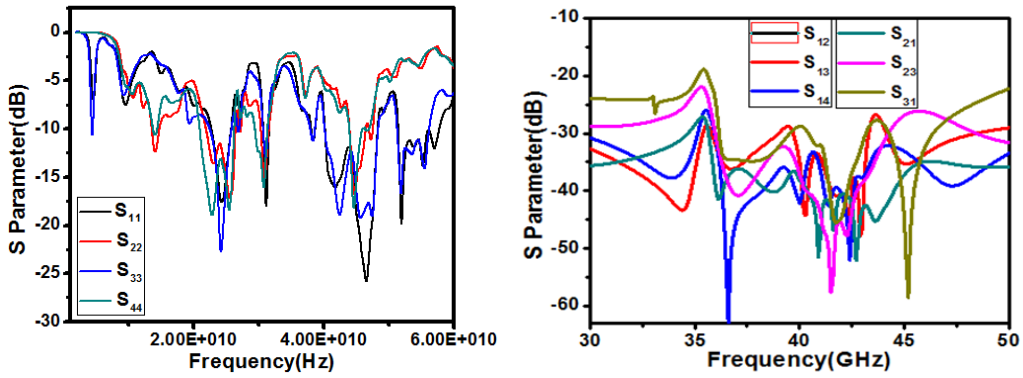

(a) (b)

Fig. 5. Measurement of S-parameters of suggested four port MIMO antenna (a) reflection coefficient (b) transmission coefficient.

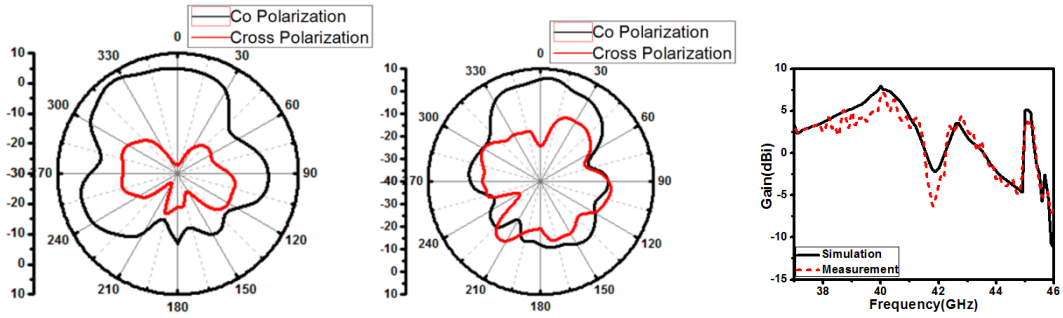

E-Plane (a) H-Plane (b)

Fig 6. Measured Result of the prototype model (a) radiation pattern at 40 GHz (b) gain.

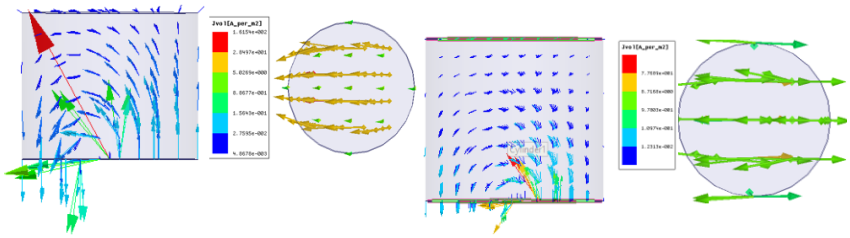

(a) (b)

Fig 7. E-field distribution at (a) 40 GHz and (b) 45 GHz.

Table 2. Comparison of earlier published work with proposed work

References	Resonant Frequency (GHz)	Type of DRA	Dimension (mm^3)	Gain (dBi)	Isolation (dB)
[12]	30	Cylindrical	48 x 21 x 3.1	7.0	-25.0
[13]	26	Rectangular	21.77 x 11x	6.4	-32.0
[14]	28	Rectangular	20 x 20 x 2.54	----	-24.0
[15]	28	Rectangular	20 x 20 x 1.6	7.5	-29.34
[16]	60.4	Cylindrical	----------	7.9	-46.5
[17]	29.4	Cylindrical	48 x 21 x 3.1	7.0	-25.0
[18]	28,38	Rectangular	25 x 15 x 1	5.8 and 7.0	-27.0
[19]	29	Rectangular	47 x 8 x 1.084	8	-20
Proposed Work	**40**	**Cylindrical**	**8 x 8 x 6**	**7.9**	**-30.0**

5. MIMO Performance Analysis

5.1. ECC and DG

ECC and DG in MIMO system can be found in two ways: by using scattering parameters [18] and by 3-D radiation patterns [19]. The mathematical relation of ECC for multiport antenna systems utilizing reflection coefficient and the radiation pattern is discretely suggested by (5) and (6).

$$ECC(\rho) = \frac{\left|s_{ii}^{*}s_{ij}+s_{ji}^{*}s_{jj}\right|}{\left(1-|s_{ii}|^{2}-|s_{ij}|^{2}\right)\left(1-|s_{ji}|^{2}-|s_{jj}|^{2}\right)} \quad (5)$$

$$ECC(\rho) = \frac{\left|\iint_{4\Pi}\left[F_i(\theta,\varphi)*F_j(\theta,\varphi)d\Omega\right]^{2}\right|}{\iint_{4\Pi}|F_i(\theta,\varphi)^{2}d\Omega|\iint_{4\Pi}|F_i(\theta,\varphi)^{2}d\Omega|} \quad (6)$$

Where $(i,j) \in \{(i,j)|1 \le i \le j \le 4, i,j \in N|\}$ and the term $F_i(\theta,\varphi)$ represents the field radiation pattern of the radiator after exciting ports i, j and the symbol * depicts the Hermitian product. This mathematical formula provides a nice projected value for an environment with rich multipath fading. Again,

DG is another vital criterion that can be visualized with ECC as in equation (7).

$$DG = 10ep \text{ and } ep = \sqrt{1 - |0.99\rho|^2} \quad (7)$$

The ECC and DG are simulated using scattering parameters, as shown in Figure 8. Ideally, ECC should be close to zero, which is offered by the proposed design. The diversity gain is also very high as desired for MIMO applications.

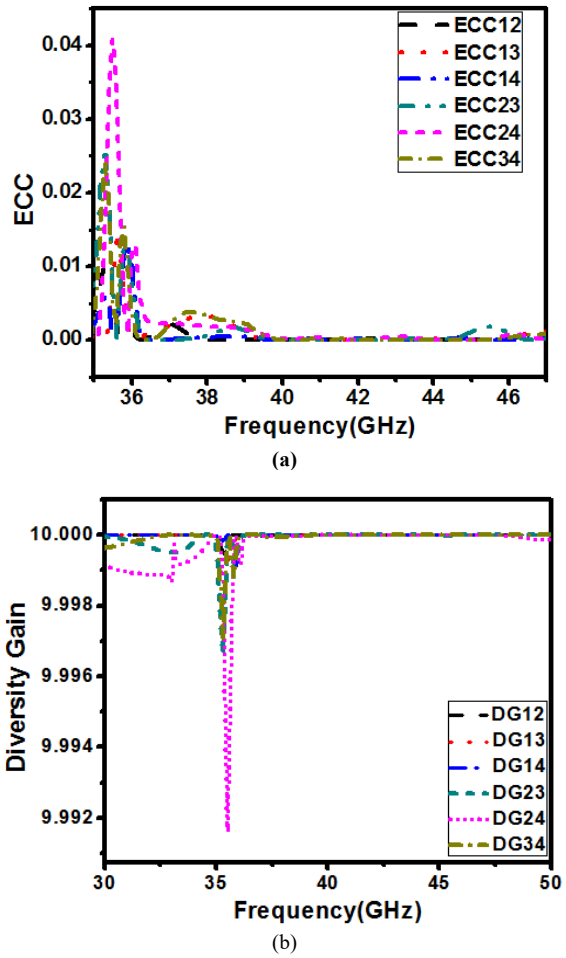

Fig. 8. The simulated results of MIMO characterization (a) ECC (b)DG

The practical implications of ECC for real world MIMO scenario should be closed to 0. For the resonance of 40 GHz, it is nearly 0 but for 45 GHz It is .005, which is very much acceptable. For the presence of great separation in radiator 3 and 4 the ECC parameter of the two ports obeys the perfect situation, i.e., lying on practically in the null line. Similarly, the DG parameters are 10 dB in every likelihood of resonance other than at 36 GHz. Ultimately the suggested MIMO antenna find perfect suitability for diversity behaviour in a multipath fading channel.

5.2 Channel capacity

The ultimate objective of MIMO configuration is to obtain the maximum permissible channel capacity [20]. Therefore, it is essential to analyse the effect of mutual coupling between the ports for achievable channel capacity in MIMO systems. Perceiving that transmitter has channel details, channel capacity of an inevitable MIMO channel is given as (8)

$$C=\log_2\left(det\left[I+\frac{SNR}{N}HH^*\right]\right) \quad (8)$$

Here I is the $N_t \times N_r$ identity matrix, $H^*$is the complex conjugate of H (the channel matrix) that is obtained by taking the S parameter after normalization, practicality at 40 GHz to determine the capacity. I refers to a 4x4 identity matrix, and H refers to a 4 x 4 S-matrix in a four-port antenna (9),

$$H=\begin{bmatrix} S_{11} & S_{12} & S_{13} & S_{14} \\ S_{21} & S_{22} & S_{23} & S_{24} \\ S_{31} & S_{32} & S_{33} & S_{34} \\ S_{41} & S_{42} & S_{43} & S_{44} \end{bmatrix} \quad (9)$$

The above equation shows the collation of the channel's capacity between one element SISO, double element MIMO and four element MIMO at 40 GHz frequency in Figure 9. A visible capacity improvement is seen in four-element MIMO than in single-element SISO and two-element MIMO with SNR.

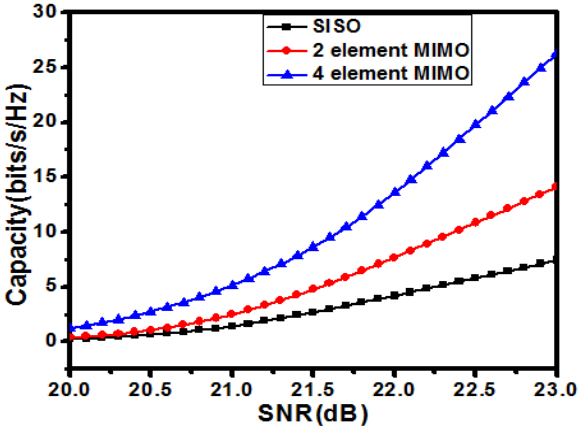

Fig. 9. Calculated channel capacity comparison at 40 GHz.

6. Conclusion

This paper designs a four-port compact integrated antenna using DRA for millimetre wave application. The design approach started by considering two ports, exciting the DRAs on a compact dielectric. With this approach, resonances at 40 and 45 GHz could be achieved. However, two port MIMO gave a gain of only 3.7 dBi. Integrating four ports on the same substrate is used to enhance the gain. An increase of gain up to 7.9 dBi is achieved with the four-port design. The transmission and reflection parameters are simulated and compared with the measured values with good agreement. The far-field radiations for the elevation and azimuth planes are also simulated and compared for the two Port and four-port MIMO configurations. The gain results at 40 GHz and 45 GHz are validated with the radiation patterns. Further, the investigation of MIMO performance parameters in terms of ECC, DG, MEG and channel capacity has validated the design approach for millimetre wave application. The antenna may find application in High-band 5G application due to excellent diversity parameters. The mathematical modelling of antenna can be developed to understand the pattern diversity of the MIMO antenna.

References

[1] Hyundong Shin and Jae Hong Lee, "Capacity of multiple-antenna fading channels: spatial fading correlation, double scattering, and keyhole," *IEEE Trans. Inform. Theory*, vol. 49, no. 10, pp. 2636–2647, Oct. 2003, doi: 10.1109/TIT.2003.817439.

[2] Q. Zhou and H. Dai, "Joint Antenna Selection and Link Adaptation for MIMO Systems," *IEEE Trans. Veh. Technol.*, vol. 55, no. 1, pp. 243–255, Jan. 2006, doi: 10.1109/TVT.2005.861211.

[3] A. Ahmad, D. Choi, and S. Ullah, "A compact two elements MIMO antenna for 5G communication," *Sci Rep*, vol. 12, no. 1, p. 3608, Mar. 2022, doi: 10.1038/s41598-022-07579-5.

[4] M. M. Fakharian, "A massive MIMO frame antenna with frequency agility and polarization diversity for LTE and 5G applications," *Int J RF Microw Comput Aided Eng*, vol. 31, no. 10, Oct. 2021, doi: 10.1002/mmce.22823.

[5] U. A. Dash and S. Sahu, "Wideband circularly polarized sectored conical dielectric resonator antenna excited by S-shaped slot," *Micro & Optical Tech Letters*, vol. 60, no. 2, pp. 310–318, Feb. 2018, doi: 10.1002/mop.30958.

[6] H. N. Chen, J.-M. Song, and J.-D. Park, "A Compact Circularly Polarized MIMO Dielectric Resonator Antenna Over Electromagnetic Band-Gap Surface for 5G Applications," *IEEE Access*, vol. 7, pp. 140889–140898, 2019, doi: 10.1109/ACCESS.2019.2943880.

[7] B. Liu, J. Qiu, N. Wang, X. Pan, J. Ni, and S. Yan, "Pyramid MIMO Dielectric Resonator Antenna with Circular Polarization Diversity," presented at the International Symposium on Antennas and Propagation (ISAP), Xi'an, China: IEEE, 2019, pp. 1–3.

[8] M. S. Sharawi, S. K. Podilchak, M. T. Hussain, and Y. M. M. Antar, "Dielectric resonator based MIMO antenna system enabling millimetre-wave mobile devices," *IET Microwaves, Antennas & Propagation*, vol. 11, no. 2, pp. 287–293, Jan. 2017, doi: 10.1049/iet-map.2016.0457.

[9] Y. M. Pan, X. Qin, Y. X. Sun, and S. Y. Zheng, "A Simple Decoupling Method for 5G Millimeter-Wave MIMO Dielectric Resonator Antennas," *IEEE Trans. Antennas Propagat.*, vol. 67, no. 4, pp. 2224–2234, Apr. 2019, doi: 10.1109/TAP.2019.2891456.

[10] A. Hassanien, W. Swelam, and M. H. A. El Azeem, "Broadband MIMO cylindrical dielectric resonator planar array antenna for millimeter-wave E-band and 5G applications," in *2018 35th National Radio Science Conference (NRSC)*, Cairo: IEEE, Mar. 2018, pp. 165–169. doi: 10.1109/NRSC.2018.8354385.

[11] M. Belazzoug, I. Messaoudene, S. Aidel, H. Boualem, Y. B. Chaouche, and T. A. Denidni, "4-port MIMO CDR Antenna based with a Defected Ground Structure for 5G mm-wave applications," in *2020 IEEE International Symposium on Antennas and Propagation and North American Radio Science Meeting*, Montreal, QC, Canada: IEEE, Jul. 2020, pp. 1367–1368. doi: 10.1109/IEEECONF35879.2020.9329706.

[12] M. T. Hussain, O. Hammi, M. S. Sharawi, S. K. Podilchak, and Y. M. M. Antar, "A dielectric resonator based millimeter-wave MIMO antenna array for hand-held devices," in *2015 IEEE International Symposium on Antennas and Propagation & USNC/URSI National Radio Science Meeting*, Vancouver, BC, Canada: IEEE, Jul. 2015, pp. 3–4. doi: 10.1109/APS.2015.7304387.

[13] A. Sharma, A. Sarkar, A. Biswas, and M. J. Akhtar, "Millimeter-Wave Quad-Port Multiple-Input Multiple-Output Dielectric Resonator Antenna Excited Differentially by TE_{20} Mode Substrate Integrated Waveguide," in *2019 URSI Asia-Pacific Radio Science Conference (AP-RASC)*, New Delhi, India: IEEE, Mar. 2019, pp. 1–4. doi: 10.23919/URSIAP-RASC.2019.8738413.

[14] Y. Zhang, J.-Y. Deng, M.-J. Li, D. Sun, and L.-X. Guo, "A MIMO Dielectric Resonator Antenna With Improved Isolation for 5G mm-Wave Applications," *Antennas Wirel. Propag. Lett.*, vol. 18, no. 4, pp. 747–751, Apr. 2019, doi: 10.1109/LAWP.2019.2901961.

[15] N. S. Murthy, "Improved isolation metamaterial inspired mm-wave mimo dielectric resonator antenna for 5G application," *PIER C*, vol. 100, pp. 247–261, 2020, doi: 10.2528/PIERC19112603.

[16] A. Dadgarpour, B. Zarghooni, B. S. Virdee, T. A. Denidni, and A. A. Kishk, "Mutual Coupling Reduction in Dielectric Resonator Antennas Using Metasurface Shield for 60-GHz MIMO Systems," *Antennas Wirel. Propag. Lett.*, vol. 16, pp. 477–480, 2017, doi: 10.1109/LAWP.2016.2585127.

[17] M. D. Alanazi and S. K. Khamas, "A Compact Dual Band MIMO Dielectric Resonator Antenna with Improved Performance for mm-Wave Applications," *Sensors*, vol. 22, no. 13, p. 5056, Jul. 2022, doi: 10.3390/s22135056.

[18] Y.-T. Liu, B. Ma, S. Huang, S. Wang, Z. J. Hou, and W. Wu, "Wideband Low-Profile Connected Rectangular Ring Dielectric Resonator Antenna Array for Millimeter-Wave Applications," *IEEE Trans. Antennas Propagat.*, vol. 71, no. 1, pp. 999–1004, Jan. 2023, doi: 10.1109/TAP.2022.3164235.

[19] D. Tse and P. Viswanath, *Fundamentals of Wireless Communication*, 1st ed. Cambridge University Press, 2005. doi: 10.1017/CBO9780511807213.

[20] F. Wang, X. Liu, and M. E. Bialkowski, "Investigation into SVD Based Beamforming over Rician MIMO Channels," in *2009 5th International Conference on Wireless Communications, Networking and Mobile Computing*, Beijing, China: IEEE, Sep. 2009, pp. 1–4. doi: 10.1109/WICOM.2009.5302947.